THE JOURNAL OF BIOLOGICAL CHEMISTRY VOL. 287, NO. 25, pp. 21396–21405, June 15, 2012
© 2012 by The American Society for Biochemistry and Molecular Biology, Inc. Published in the U.S.A.

Obstructor-A Is Required for Epithelial Extracellular Matrix Dynamics, Exoskeleton Function, and Tubulogenesis*[S]

Received for publication, March 7, 2012, and in revised form, April 17, 2012 Published, JBC Papers in Press, April 27, 2012, DOI 10.1074/jbc.M112.359984

Georg Petkau, Christian Wingen, Laura C. A. Jussen, Tina Radtke, and Matthias Behr[1]

From the Life & Medical Sciences Institute (LIMES), Laboratory for Molecular Developmental Biology, University of Bonn, Carl-Troll-Strasse 31, 53115 Bonn, Germany

Background: The extracellular matrix (ECM) is essential for protection and development of epithelial tissues.
Results: Obstructor-A (Obst-A) organizes a core complex with chitin modifiers and enzymes to protect ECM from premature degradation.
Conclusion: Obst-A is required for growth control, tubulogenesis, wound healing, and epithelial integrity.
Significance: This novel mechanism is crucial for understanding ECM dynamics of epithelial tissues.

The epidermis and internal tubular organs, such as gut and lungs, are exposed to a hostile environment. They form an extracellular matrix to provide epithelial integrity and to prevent contact with pathogens and toxins. In arthropods, the cuticle protects, shapes, and enables the functioning of organs. During development, cuticle matrix is shielded from premature degradation; however, underlying molecular mechanisms are poorly understood. Previously, we identified the conserved *obstructor* multigene-family, which encodes chitin-binding proteins. Here we show that Obstructor-A is required for extracellular matrix dynamics in cuticle forming organs. Loss of *obstructor-A* causes severe defects during cuticle molting, wound protection, tube expansion and larval growth control. We found that Obstructor-A interacts and forms a core complex with the polysaccharide chitin, the cuticle modifier Knickkopf and the chitin deacetylase Serpentine. Knickkopf protects chitin from chitinase-dependent degradation and deacetylase enzymes ensure extracellular matrix maturation. We provide evidence that Obstructor-A is required to control the presence of Knickkopf and Serpentine in the extracellular matrix. We propose a model suggesting that Obstructor-A coordinates the core complex for extracellular matrix protection from premature degradation. This mechanism enables exoskeletal molting, tube expansion, and epithelial integrity. The evolutionary conservation suggests a common role of Obstructor-A and homologs in coordinating extracellular matrix protection in epithelial tissues of chitinous invertebrates.

In arthropods the cuticle covers the body and internal organs. The cuticle is important, since it plays key roles in growth control, wound healing, and environmental protection (1–3). During development, cuticles undergo several rounds of molting to overcome size limitations. This process requires the coordinated secretion and assembly of new cuticles and the replacement of old ones (2–4). The polysaccharide chitin is an important cuticle matrix component that together with proteins and lipids forms highly organized and abundant extracellular matrices (ECM)[2] in arthropods and nematodes. Previous studies of the *Drosophila* embryonic tracheal system investigated the biosynthesis and secretion of the apical chitin ECM into newly formed tube lumina (reviewed in Refs. 4–6). Additionally, chitin matrix formation in the embryonic tracheal cuticle involves Knickkopf (Knk) a conserved GPI-linked chitin-binding protein. Knk has been characterized in *Drosophila* and in *Tribolium* (7, 8). It acts in the newly synthesized cuticle where it is involved in chitin organization and protects chitin from chitinases-mediated degradation. Down-regulation of *knk* resulted in a chitinase-dependent chitin reduction, lethality and severe molting defects (8). Cuticle maturation involves the deacetylation of chitin, organizing physical and chemical properties of the ECM. Chitin deacetylase-like proteins are conserved and homologs have been found in insects (9). In *Drosophila* the deacetylation domain proteins Serpentine (Serp) and Vermiform (Verm) are essential for cuticle function. They preserve the chitin texture in the new tracheal cuticle as well as in the epidermal cuticle (10, 11).

Although single proteins involved in chitin matrix assembly and modifications were identified, little is known about the organization of chitin dynamics. In this study we identified a molecular mechanism that protects the apical ECM from premature degradation in *Drosophila*. This mechanism is controlled by Obstructor (Obst)-A, encoded by a member of the previously identified *obstructor* (*obst*) multigene family (12). We show that Obst-A binds chitin and interacts with Knk and Serp. The resulting chitin protein complex organizes and protects chitin from premature degradation. This is essential for cuticle function and molting.

* This work was supported by the German Research Foundation (Deutsche Forschungsgemeinschaft, SFB645) (to M. B.) and by the Boehringer Ingelheim Fonds (to C. W.).
[S] This article contains supplemental Figs. S1–S7, Materials and Methods, and References.
[1] To whom correspondence should be addressed. Tel.: 49-228-7362746; Fax: 49-228-7362643; E-mail: mbehr@uni-bonn.de.

[2] The abbreviations used are: ECM, extracellular matrix; Obst, Obstructor; AEL, after egg laying; Hsc, heat shock cognate; Serp, Serpentine; Verm, Vermiform; KnK, Knickkopf; CBD, chitin-binding domain; Cbp, chitin-binding-probe; st, stage; WGA, wheat germ agglutinin.

EXPERIMENTAL PROCEDURES

Fly Stocks—Bloomington/Harvard stock centers: w^{1118} (referred to as *wt*), *breathless*GAL4; RBe03601, WHf02348, WHf03687 were used to generate *obst-A*-null mutants according to Ref. 13; *serp verm* double mutants (10); UAS-Cht2 (14). Balancer strains with *GFP* or *lacZ* transgenes were used to identify genotypes. Thus, *obst-A* alleles were kept either with the FM7i,P{ActinGFP} or the FM7c,P-{ftz/lacZ} balancer chromosome. In contrast to control animals, hemizygous mutants do not express GFP or β-galactosidase. This allows the identification of hemizygous *obst-A* mutants.

Immunolabeling and Binding Assays—Fixation and immunolabeling were performed as described in Ref. 15. The anti-Obst-A antibody against the C-terminal peptide was generated in rabbits. After final bleeding, the anti-Obst-A antibody was affinity-purified from the sera by using the C-terminal peptide (Eurogentech, Brussels, Belgium). We used anti-Obst-A (1:50), anti-Knk, anti-Serp, Cbp, WGA (all 1:100 in embryos) and anti-α-Spectrin (1:10) for immunolabeling. Primary antibodies were detected by secondary antibodies obtained from Molecular Probes (Alexa488-, Alexa546-, or Alexa633-conjugated) and Dianova (JacksonImmuno, Westgrove, Cy2-, Cy3-conjugated). After washing, embryos were mounted in Vectashield (Vector Laboratories, Burlingame). Fluorescein conjugated chitin-binding probe (Cbp, 1:100, New England BioLabs, Ipswitch) detects chitin and Alexa633-conjugated wheat germ agglutinin (WGA, 1:100; Molecular Probes, Invitrogen, Carlsbad) selectively recognizes *N*-acetylneuraminacid and *N*-acetylglucosamine sugar residues at the plasma membrane surface. Immunolabeling was detected and analyzed by a Zeiss LSM 710 (Zeiss, Oberkochen, Germany) confocal microscope (ZEN software; sequential scans). For confocal images pinhole "airy unit 1" Zeiss standard settings were used to receive signals only from the focal plane. Each fluorochrome was scanned individually in single optical sections ("sequential scan") to avoid cross-talk between channels. Subcellular studies were analyzed using a Zeiss 63× LCI Plan Neofluar objective and the Zeiss-Zen software. Images were cropped in Adobe Photoshop CS5 and figures designed with Adobe Illustrator CS5.

For generating the GST-Obst-A fusion protein, we cloned a full-length *obst-A* open-reading frame PCR product in-frame in the pGEX-4T-3 vector. The following primer pair was used: AACCGAATTCCATGAAGTTATTTTTATGTG; GATTGCTCGAGTCTTAGTCCTTCTT. The construct was tested by sequence analysis and transformed into *Escherichia coli* BL21 cells for isopropyl β-D-1-thiogalactopyranoside (IPTG) induction (4 h at 27 °C) of the GST-Obst-A fusion protein, which was purified by using GST beads. Samples were subjected to SDS-PAGE and transferred to an Immobilon-P membrane (Amersham Biosciences, GE Healthcare, Little Chalfont), blocked for 1 h with Roti-block (Roth, Karlsruhe, Germany) and incubated overnight (4 °C) with the primary antibody. Horseradish peroxidase (HRP)-conjugated secondary antibody was used for chemiluminescent detection (ECL, Pearce, Thermo Scientific, Rockford). Serp,Verm, Knk were used in a 1:1000 and Obst-A in a 1:5000 dilution.

Colloidal Chitin Binding Assay—The colloidal chitin-binding assay was previously reported (16). 0.5 ml chitin-beads (New England BioLabs, Ipswich) were incubated in 0.5 ml Hepes and 230 μg of embryo extract (23 μg/μl) overnight at 4 °C, washed afterward 20 times with 0.5 ml of Hepes, and five times with PBS. Bound proteins were incubated for 15 min in 0.5 ml Hepes and 0.1 ml elution buffer (80% SDS buffer and 20% β-mercaptoethanol) for elution. Samples were subjected to SDS-PAGE and transferred to an Immobilon-P membrane (Amersham Biosciences, GE Healthcare, Little Chalfont) and probed with anti-Obst-A (1:4000) and anti-Hsc70 (1:1000) antibodies.

Cuticle and Nikkomycin Assays—Flies were fed 2 days with a mixture of Nikkomycin-Z (Sigma, 0.5 mg/ml) and yeast paste to collect chitin reduced embryos, according to Refs. 7, 14. For cuticle integrity assay larvae were pricked with a glass needle and monitored with an Olympus AX70. For cuticle preparation, larvae were selected for genotype, washed with H_2O, and incubated in 1:1 lactate and Hoyers reagent overnight at 65 °C. Larval stages were determined by morphology of mouth-hooks. Small and one-toothed mouth hooks are characteristic for first instar larvae. About 48 h, after egg laying (AEL) the first instar larvae molt to second instar, which can be identified by a mouth-hook with two to five teeth. For the analysis of the tracheal cuticle we used living larvae mounted in Olympus immersion oil. Larvae were analyzed with 100× objective and Nomarski microscopy (DIC; Olympus AX70, Tokyo, Japan). Images were generated with Cell'F and cropped with Adobe Photoshop CS5.

Accession Numbers of Obst-A Homologs—*Acromyrmex echinatior*, "leaf-cutter" ant (EGI67437), *Acyrthosiphon pisum*, pea aphid (NP_001156724; synonym Ap-A1), *Aedes aegypti*, yellow fever mosquito (XP_001662353; Aa-24), *Anopheles gambiae*, Malaria mosquito (XP_309184; Ag-989), *Apis mellifera*, honey bee (XP_001120217; Am-A), *Bombus terrestris*, bumblebee (XP_003394171), *Caenorhabditis elegans*, worm (W03F11.1), *Culex quinquefasciatus*, southern house mosquito (XP_001842244; Cq-A1), *Drosophila melanogaster*, fruit fly (NP_608378), *Heliconius melpomene*, postman butterfly (AEU11713), *Ixodes scapularis*, deer tick (XP_002413846), *Pediculus humanus corporis*, head louse (XP_002429481; Pc-A), *Nasonia vitripennis*, parasitic wasp (NP_001165855; Nv-A1), *Tribolium castaneum*, red flour beetle (NP_001161910; CPAP-3A1).

RESULTS

Obst-A Is Essential for Larval Growth and Cuticle Molting—*Drosophila* larvae dramatically increase their body size during development. Searching for mutants causing early lethality and body size reduction (Fig. 1, *A* and *B*), we identified a P-element ($obst\text{-}A^{663}$) inserted upstream of the *obst-A* (CG17052; Fig. 2*A*; supplemental Fig. S1, *A* and *B*) gene at the X-chromosome (19C1).

To investigate developmental functions of the *obst-A* gene, two *obst-A*-null mutants ($obst\text{-}A^{d02}$, $obst\text{-}A^{d03}$) were generated (Fig. 2*A*) using the FLP-FRT based technique (13). Additionally, we identified a deficiency mutant (Df(1)HM44), which lacks *obst-A*. All identified alleles cause lethality of hemizygous

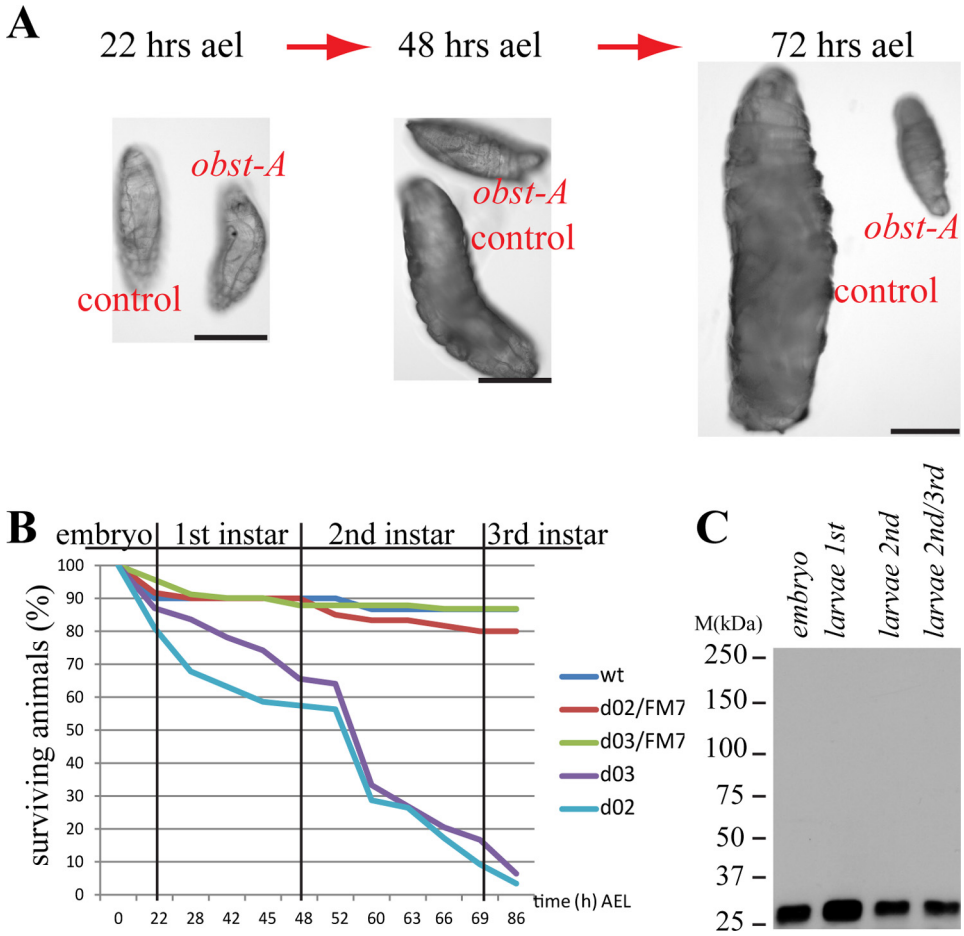

FIGURE 1. **Obst-A is essential for larval growth and survival.** *A*, brightfield microscopy images of *obst-A*-null mutants and heterozygous control larvae. *obst-A* mutant larvae fail to increase their body size, when compared with control animals. Scale bars, 0.5 mm. *B*, survival tests revealed larval lethality of *obst-A*-null mutants, but not for *wt* and control animals (0–86 h after egg laying (AEL); *obst-A*^{d02} $n = 137$; *obst-A*^{d03} $n = 128$, *wt* $n = 30$; heterozygous *obst-A*^{d02}/FM7 $n = 60$; heterozygous *obst-A*^{d03}/FM7 $n = 91$). *C*, immunoblot treated with the anti-Obst-A antibody detects Obst-A (~26,5kDa predicted) in *wt* embryo and larval extracts.

mutant animals (not shown; see below). Trans-heterozygous mutants combining heterozygous alleles of *obst-A*^{663}, *obst-A*^{d02}, *obst-A*^{d03}, and the deficiency were lethal and showed that the *obst-A* mutations did not complement each other (supplemental Fig. S2*A*). We generated a transgenic UAS-*obst-A* fly line for GAL4 driven *obst-A* overexpression. The ectopic expression of *obst-A,* was able to rescue *obst-A*-null and P-element induced lethality (supplemental Fig. S2*B*). In summary, complementation and rescue studies identified *obst-A*^{d02}, *obst-A*^{d03}, and *obst-A*^{663} as *obst-A* alleles.

Northern blot analysis identified two *obst-A* transcripts (supplemental Fig. S1*C*). Both transcripts encode for a single putative protein with a predicted size of 27 kDa (12). To analyze the *obst-A* gene product, we raised a specific antibody that recognizes the C terminus of Obst-A (Fig. 2*A*). Immunofluorescent stainings showed that the antibody specifically recognizes UAS-GAL4 mediated ectopic Obst-A expression in whole mount embryos (supplemental Fig. S1, *D* and *E*). In confocal studies of whole mount embryos the anti-Obst-A antibody detects a specific pattern, which was absent in the *obst-A* deletion mutants (supplemental Fig. S1, *F–H*). On immunoblots, the anti-Obst-A antibody detects a prominent signal at the expected size of 27 kDa of *wild-type* (*wt*) but not of *obst-A* deficiency and null mutant extracts (supplemental Fig. S1, *I–K*).

To assess the *obst-A* importance for development, we monitored the P-element and deletion mutants by Nomarski microscopy. All *obst-A* mutants failed in body size expansion during larval development, while control animals and heterozygous siblings doubled or even tripled their body size at the same time (Fig. 1*A*; supplemental Fig. S2, *C* and *C′*). Additionally, the *obst-A*-null mutation caused larval lethality (Fig. 1*B*), which was rescued to adulthood by UAS-GAL4-mediated Obst-A overexpression using either ubiquitous or ectodermal specific driver lines (supplemental Fig. S2*B*). Immunoblot analysis of *wt* animals, using the specific anti-Obst-A antibody, identified Obst-A in embryonic and larval stages (Fig. 1*C*). These findings provide evidence for a vital role of Obst-A during larval development and body size control.

Defective food passage from the foregut into the midgut can result in larval lethality (17). We performed a feeding assay using Carmine Red (Sigma) labeled yeast paste and monitored its passage into larval midgut by bright field microscopy. The *obst-A*-null mutant larvae were lethargic compared with control animals, but crawled and ingested red labeled food, which

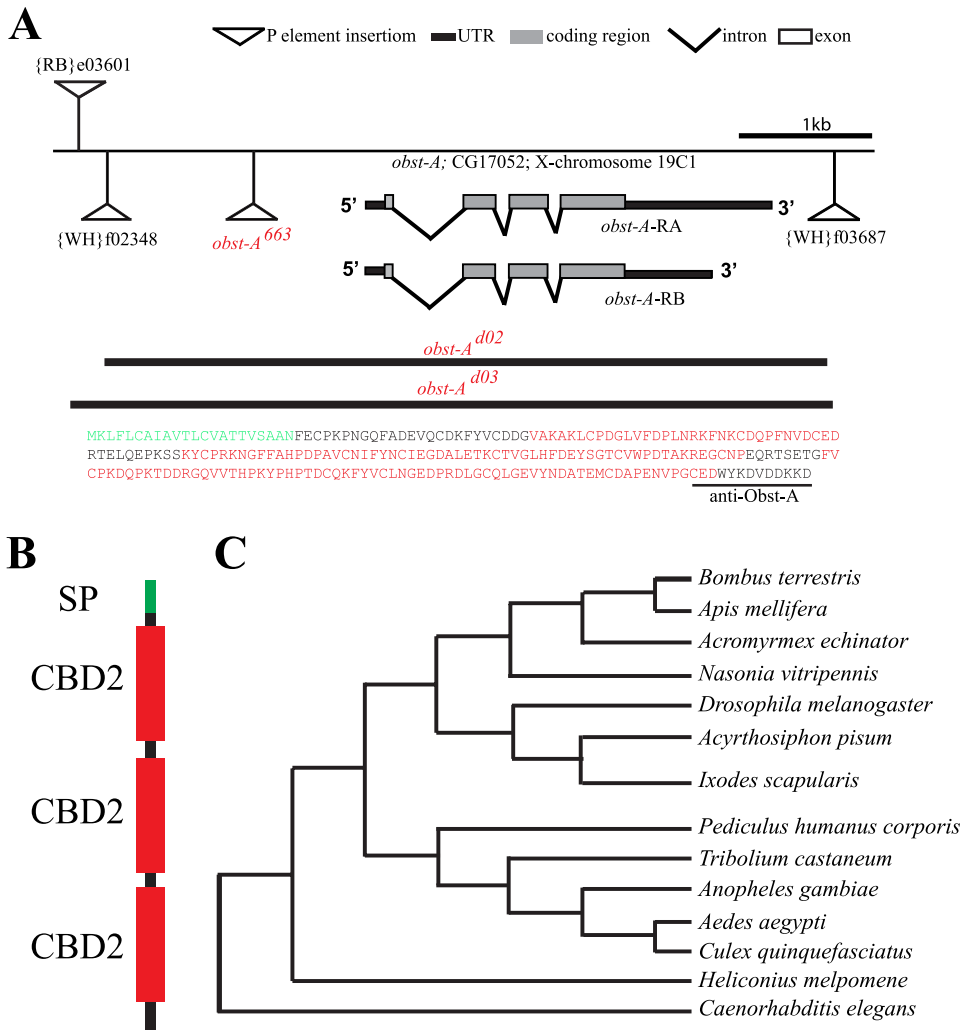

FIGURE 2. **Obst-A is a conserved chitin-binding domain protein with putative homologs among arthropods and nematodes.** *A*, molecular organization of the genomic region 19C1 containing the *obst-A* gene. Insertions of the *obst-A*^{663} P-element and the PiggyBac transposons, used for generation of *obst-A*^{d02} and *obst-A*^{d03} deletion mutants (*black lines below* indicate the deleted regions), are indicated. *Gray bars* show the open reading frame, which is similar in both *obst-A* transcripts. Supporting information, such as Northern blot analysis, is provided in supplemental Fig. S1C. In the deduced Obst-A amino acid sequence (237 aa, MW: 26.5kDa) the N-terminal signaling peptide is indicated in *green* and the three type 2 chitin-binding-domains in *red*. The *underlined sequence* at the C terminus shows the peptide used to generate the anti-Obst-A antibody. *B*, diagram shows the signaling peptide (SP, *green*), chitin-binding domains (CBD2, *red*) and a C-terminal stretch of Obst-A. Domains were annotated with the SMART database and the SignalP 4.0 Server. *C*, phylogenetic analysis of Obst-A sequence identified homologs in different nematodes and arthropods (accession numbers see supplement; MEGA 5.0 alignment).

was predominantly found in the midgut and indistinguishable from control animals (supplemental Fig. S2*D*). This suggests that food passage was not affected.

Protein domain predictions of Obst-A amino acid sequence revealed a signal peptide and three chitin-binding domains type 2 (ChtBD2; Fig. 2*B*), spaced by two linker regions (12). We screened available databases and blast search programs with standard settings, provided by the NCBI, and used the Mega5 (18) software for protein alignments. We identified Obst-A homologs among arthropods, such as bugs, ticks, mosquitoes, and nematodes (Fig. 2*C*), but not in fungi or plants. The conserved sequence and domain arrangements of chitin-binding domains suggest a common role of Obst-A and its homologs in the organization of chitinous cuticles. Previously, larval lethality and body size arrest have been linked to cuticle molting defects, where mutant larvae possessed old and new cuticles (19). Preparation of *obst-A* mutant cuticles of late embryos revealed normal structure (supplemental Fig. S3, *A–D*). In contrast, cuticle preparation of larvae, containing second instar multiple teethed mouth hooks, showed severe defects in *obst-A* mutants. While control animals replaced their cuticle (Fig. 3, *A-A″*; supplemental Fig. S3, *E, G, I, I′*), *obst-A* mutant larvae showed cuticle molting defects of head skeleton, epidermis, tracheae, and posterior spiracles (Fig. 3, *B-B″*; supplemental Fig. S3, *F, H, J*). The tracheal cuticle was analyzed *in vivo* by Nomarksi optic using first instar larvae shortly and 24 h after hatching, when they started to molt into second instar. Analysis of the tracheal cuticle revealed in early and late first instar control animals regularly spaced taenidial folds, thickenings in the inner tube surface. In contrast, *obst-A* mutants showed misarranged taenidial folds (Fig. 3, *C-D′*). In summary, this indicates that Obst-A is required for taenidial arrangement and cuticle molting since old cuticles are not properly degraded. It further suggests that Obst-A controls body size by its effect on cuticle molting.

To test the protective function of the epidermal cuticle, its integrity was studied. This assay was adapted to a previous pub-

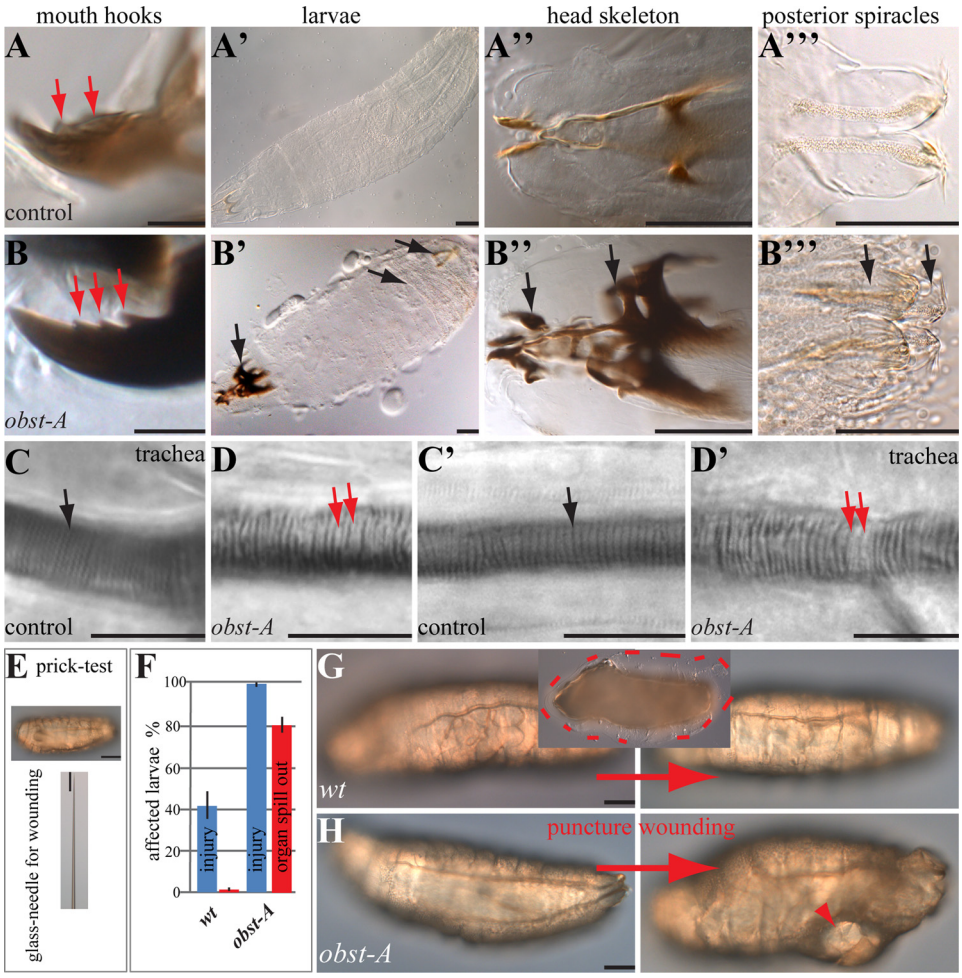

FIGURE 3. **Obst-A is required for cuticle integrity and function.** Nomarski-optic images of larvae. *A-B‴*, cuticle preparations of 60 h AEL *obst-A* heterozygous control animals (*A-A‴*), and *obst-A*-null mutants (*B-B‴*) showed multiple teethed (*red arrows*) mouth hooks, which is characteristic for second instar larvae. In contrast to control animals, *obst-A*-null mutants possess old and new cuticles (indicated by arrows) of head skeleton, epidermis (see supplemental Fig. S3, *E* and *F*) and posterior spiracles. Note the strong darkening of the head skeleton. *C-D′*, *in vivo* Nomarski microscopy of first instar larvae shortly after hatching (*C*, *D*) and 48 h AEL (*C′*, *D′*). Control animals (*C*, *C′*) show regularly spaced taenidial folds (*black arrows*). The *obst-A* mutants (*D*, *D′*) show defects (*red arrows* point to gaps) of taenidial fold arrangement. Taenidia of *obst-A* mutant early first instar larvae show in addition unusual strong light refraction when compared with the thin taenidial folds of control animals. *E–H*, cuticle integrity assay of first instar larvae. *E*, larvae were pricked laterally with a glass-needle, normally used for microinjection. *F*, histogram indicates injured larvae after puncture wounding in percentage, $n = 17$ for *wt* and $n = 20$ for *obst-A*-null mutants. Bars show standard deviation. *G*, *wt* larva before (*left*) and after (*right*) wounding. No profound injury is observed, only little hemolymph oozes out (framed by the *red dashes* in the inlay image). *H*, in contrast, most of the *obst-A*^{d03} mutant larvae show severe injuries (*arrowhead*), as vital organs spilled out. Scale bars represent 10 μm in *A*, *B*, *C-D′* and 100 μm in others.

lication, demonstrating larval wound healing after stabbing of animals (1). We gently pricked first instar larvae with a thin glass needle normally used for microinjection and immediately monitored them by Nomarski microscopy (Fig. 3*E*). Most of the *wt* larvae showed no injury after pricking and only about 40% began to bleed slightly (Fig. *3*, *F* and *G*). In contrast, all pricked *obst-A* mutants bled strongly, organs spilled out and they died within a few minutes (Fig. 3, *F* and *H*). The phenotypes caused by epidermal rupture of mutant larvae suggest that Obst-A is involved in epidermal body protection, provided by the cuticle.

Chitin Associates with Obst-A and Controls Its Localization—The three identified putative Obst-A chitin-binding domains suggest a chitin interaction. This was addressed by a chitin-binding assay. We used a colloidal chitin-bead affinity chromatography (see "Experimental Procedures"). In this assay Obst-A was pulled down by colloidal chitin from embryo extract, but not the intracellular protein heat shock cognate (Hsc) 70 as a negative control (Fig. 4*A*). This indicates that Obst-A interacts with chitin. Additionally, immunofluorescent confocal studies in whole mount embryos revealed Obst-A transcript and protein expression in cuticle forming organs, predominantly in tracheae, foregut, posterior spiracles, and epidermis (Fig. 4, *B–D*; supplemental Fig. S3, *K* and *L*). In *Drosophila* embryos chitin can be visualized by the fluorescein-linked chitin-binding-probe (Cbp). Confocal studies of immunostainings in *wt* embryos showed co-localization of Obst-A and chitin at the epidermal surface (Fig. 4*E*) and in the tracheal tube lumina (Fig. 4, *G* and *H*; supplemental Fig. S4). Next, we tested whether chitin has any effect on Obst-A localization. Flies fed with nikkomycin (7, 14), a competitive chitin synthase inhibitor, produced offspring with strong embryonic chitin reduction in the epidermis and tracheal lumina (Fig. 4, *F*, *I*). Importantly, this led to reduction and mislocalization of extracellular Obst-A (Fig. 4, *F*, *I*). Chitinases are conserved members of a hydrolase family

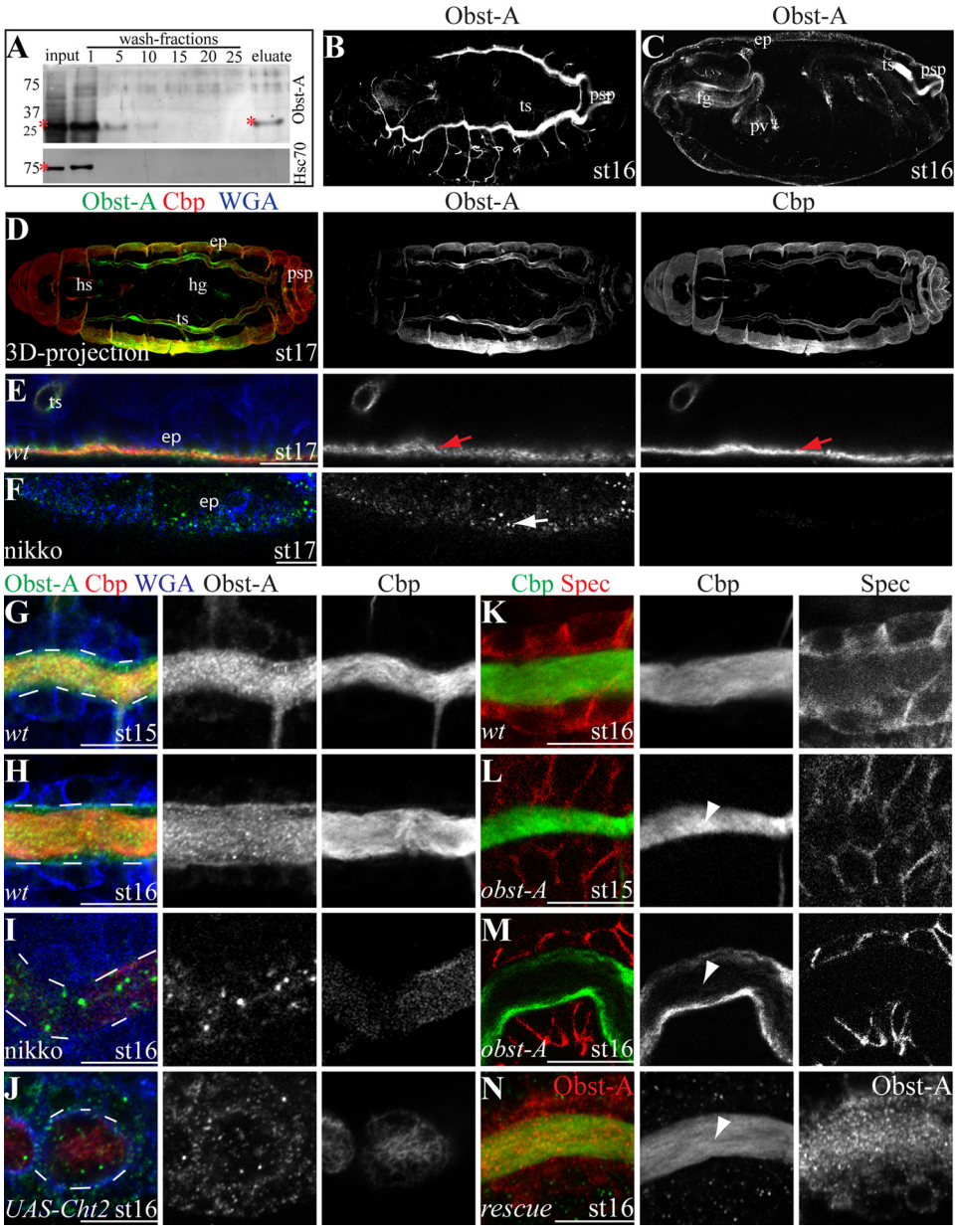

FIGURE 4. **Obst-A binds and protects chitin from premature degradation in the cuticle.** *A*, chitin-binding assay using a chitin-column and embryonic protein extract. The anti-Obst-A detects Obst-A in the input and in the eluate. The anti-heat shock cognate (Hsc) 70 antibody was used as a negative control and did not detect Hsc70 in the eluate. *Asterisks* indicate Obst-A and Hsc70. *B-N*, confocal microscopy using Cbp, WGA, the anti-Obst-A, and anti-α-Spectrin antibodies. Cbp vizualizes chitin, WGA labels cell surfaces, and Spectrin cell membranes. *B-D*, St16 and st17 (three-dimensional (3D) projection) embryos reveal Obst-A expression in the tracheal system (*ts*), the foregut (*fg*) including the proventriculus (*pv*), the posterior spiracles (*psp*), the hindgut (*hg*), head skeleton (*hs*), and the epidermis (*ep*). *E*, *F*, in st17 embryos, Obst-A co-localizes with chitin at the apical surface of epidermal cells (*arrows* in *E*) but is mislocalized (*arrow* in *F*) when chitin is strongly reduced due to nikkomycin (*nikko*) treatment. *G–J*, in st15 and st16 *wt* embryos, Obst-A accumulates and co-localizes with chitin in the tracheal tube lumen (*G*, *H*), but is mislocalized when chitin is strongly reduced due to nikko treatment (*I*) or by tracheal specific (*breathless*GAL4 driver line) overexpression of UAS-Cht2 transgene (*J*). *White dashes* indicate the tracheal lumen. *K*, in st16 *wt* embryos chitin is accumulated in the tracheal lumen. *L*, *M*, in st15 *obst-A*-null mutant chitin accumulated in the tracheal lumen but appeared strongly reduced in st16 (*arrowheads*). *N*, tracheal specific Obst-A expression using a UAS-*obst-A* transgene and the *breathless*GAL4 driver line rescued *obst-A*-null mutant tracheal chitin reduction defects. In rescued embryos chitin (Cbp, *green*; Obst-A, *red*) accumulated and is present in st16 embryos (*arrowhead*). Single channels are indicated in *gray*. Scale bars represent 10 μm.

mediating chitin digestion (20). Tracheal overexpression of the Chitinase2 (Cht2) reduced chitin levels, which resulted in Obst-A reduction and mislocalization (Fig. 4*J*). Altogether, our data provide evidence, that Obst-A is co-expressed, co-localized and associated with chitin. It further shows that chitin is required for cuticular Obst-A localization.

Obst-A Prevents Premature Chitin Degradation—Cuticle molting defects in the mutants and chitin binding suggest an unknown and important role of Obst-A in organization of chitin dynamics. In order to assess the role of Obst-A in chitin assembly or degradation, we studied chitin in the tracheal lumina of late embryos. For this assay we used the chitin marker Cbp and confocal microscopy. In *wt* embryos chitin strongly accumulates in the tracheal lumina (Fig. 4, *G*, *H*, *K*; supplemental Fig. S4, *A–C*) from stage (st)14 onwards, and is degraded at st17 (supplemental Fig. S4, *D*, *D′*) (21–23). *obst-A* mutant

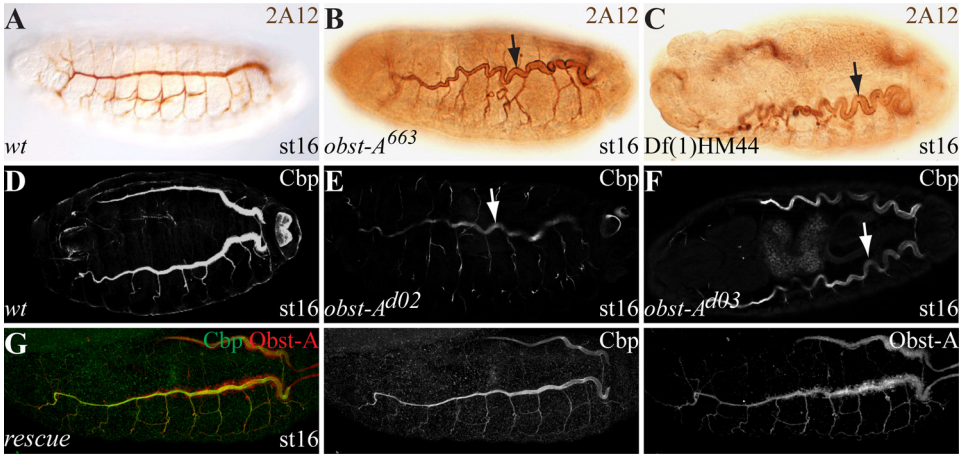

FIGURE 5. **Obst-A is required for tube size control.** Immunohistochemical stainings (*A–C*) and confocal images (*D–G*) show st16 embryos. The anonymous 2A12 antibody (*A–C*) was used for detecting tracheal tube lumina, the chitin-binding probe (*Cbp*) to visualize chitin (*D–G*). *A–C*, *wt* embryos show straightly formed tracheal tubes (*A*). *obst-A*^{663} P-induced and *obst-A* deficiency mutants show convoluted trachea (*arrows* in *B*, *C*). *D–F*, in *wt* embryos Cbp labeling revealed chitin accumulation in the tube lumina organizing a chitin cable, which is required for uniform tube expansion and tube size restriction. In contrast, in st16 *obst-A*^{d02} and *obst-A*^{d03}-null mutants, chitin appeared strongly reduced in the tube lumina. This results in tube overexpansion, which is characterized by convoluted trachea (*arrows* in *E*, *F*). *G*, *obst-A* mutant tube size defect was rescued by tracheal specific Obst-A expression (detected by anti-Obst-A, *red*) using a UAS-*obst-A* transgene and the *breathless*GAL4 driver line. Rescue embryos show straight tracheal tubes. Single channels are indicated in *gray*.

embryos accumulated chitin in the tracheal lumina until st15 (Fig. 4*L*). This, in combination with the ultrastructure analysis (supplemental Fig. S5, *A–D*), shows that Obst-A is not involved in cuticle synthesis, secretion, and assembly. In contrast to *wt*, *obst-A* mutants showed irregular chitin degradation in the tracheal lumina at st16 (Fig. 4*M*). At st16 of embryogenesis, the chitin ECM structure restricts tube size expansion (10, 11). We analyzed st16 trachea by confocal and bright field microscopy. In contrast to *wt*, the *obst-A* mutants showed convoluted trachea, which appear when tube size is strongly elongated (Fig. 5, *A–F*, supplemental Fig. S5, *E* and *F*). Tracheal specific Obst-A expression in *obst-A* mutant embryos rescued the st16 chitin degradation and tube size defects (Figs. 4*N* and 5*G*). These findings indicate that Obst-A is required to prevent existing chitin from premature degradation, which is essential in the trachea to determine tube size.

Obst-A involvement in protecting tracheal chitin from degradation, may have further consequences for the epithelial integrity. The diffusion of rhodamine-conjugated dextran (10 kDa) can be observed when the trans-epithelial barrier is defective in mutants affecting septate junctions formation (24, 25). We injected dextran into the body cavity of living embryos at st16, when the tracheal chitin ECM in *obst-A*-null mutants is reduced. In *wt* and control animals dextran was not visible in the tracheal lumina (supplemental Fig. S5, *A*, *K*). In contrast, dextran was detectable in the lumina of ~80% of *obst-A* mutants (supplemental Fig. S5, *H–K*). However, dextran diffusion in *obst-A* mutants is not as penetrant as observed in mutants affecting septate junctions (24, 25). This indicates that Obst-A is not involved in septate junction formation and the associated paracellular barrier formation. The mild diffusion phenotype of *obst-A* mutants could be induced by the fragility of the defective luminal matrix as observed in the epidermal integrity test.

Obst-A Forms a Complex with Knk and Serp to Prevent Premature ECM Degradation—To understand the molecular role of Obst-A in organizing ECM dynamics, essential components of the chitin matrix were studied. Serp and Verm modify and preserve the texture of luminal chitin in the embryonic tracheae (10, 11). In immunofluorescent labeling studies, we tested whether Obst-A localization requires Serp and Verm. In *serp verm* double mutants, extracellular Obst-A accumulated in the tracheal lumina but appeared mislocalized and grainy compared with *wt* (supplemental Fig. S5, *L–O*). The involvement in proper Obst-A localization in the tracheal lumina, prompted us to ask whether Serp and Verm may interact with Obst-A. Thus, interaction assays were performed using a glutathione *S*-transferase (GST)-tagged Obst-A fusion protein. This fusion protein was recognized by the anti-Obst-A and anti-GST antibodies (supplemental Fig. S6*A* and control experiments in Fig. 6, *A* and *B*; supplemental Fig. S6). For these assays, GST-Obst-A fusion protein and GST alone, as a negative control, were purified with GST beads from bacterial lysate. As expected, GST alone did not pull down Serp or Verm from embryo lysate. In contrast, the GST-Obst-A fusion protein pulled down specifically Serp but not Verm (Fig. 6*A*; supplemental Fig. S6, *B* and *C*). Both, Serp and Verm contain a chitin-binding domain (10, 11), suggesting that they may interact with chitin. To exclude indirect co-precipitation due to possible Serp chitin interaction, we tested the pull down with embryo lysate where chitin was strongly reduced by nikkomycin treatment (see Fig. 4, *F*, *I*). This confirmed the co-precipitation of GST-Obst-A with Serp (Fig. 6*B*; supplemental Fig. S6, *B′*).

Next, we tested by confocal analysis whether Serp localization involves Obst-A. In *wt* embryos, Serp accumulated in the tracheal lumina from st14 until st16 (Fig. 6, *C* and *D*; supplemental Fig. S7, *A* and *B*). In contrast, although accumulation was normal at st14 and 15, luminal Serp degraded in *obst-A* mutants from late st15 onwards and appeared strongly reduced at st16 (Fig. 6, *E* and *F*; supplemental Fig. S7, *C–E*). These findings show that Obst-A is not involved in the secretion and assembly but is required for Serp presence in the chitin ECM of tracheal tubes. The immunostainings further suggest that Serp degradation can be independent of chitin in *obst-A* mutants.

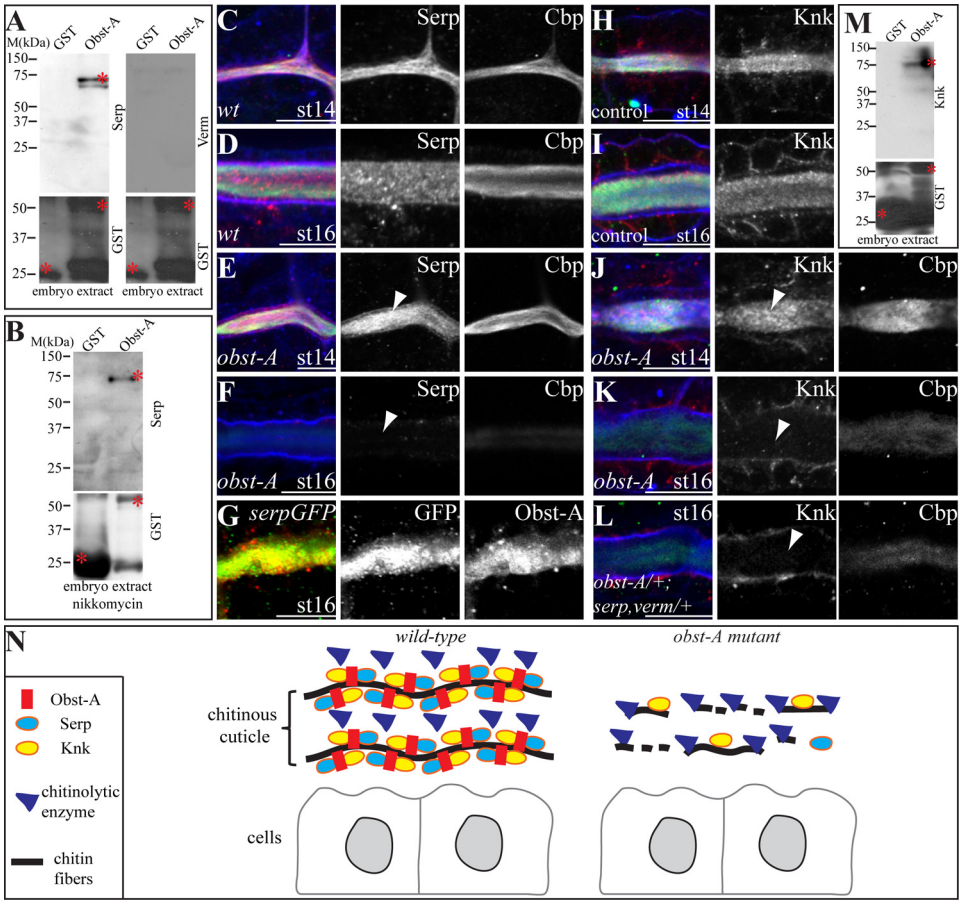

FIGURE 6. **Obst-A interacts with Serp and Knk to coordinate their localization in the cuticle.** *A* and *B*, *in vitro* interaction assay; Serp but not Verm is specifically pulled down from *wt* embryo extracts and from chitin reduced extracts (nikkomycin treatment) by Obst-A fused to GST. GST was used as a negative control. *Asterisks* mark GST, GST-Obst-A, and Serp proteins. *C–L*, confocal images showing magnifications of tracheal tubes using Cbp, WGA and anti-Obst-A, anti-GFP, anti-Serp, and anti-Knk antibodies. *C* and *D*, in st14 and st16 *wt* embryos, Serp is enriched in the tracheal lumen. *E* and *F*, in st14 *obst-A*-null mutant embryos Serp is accumulated in the tracheal lumen, but luminal Serp is reduced at st16 (*arrowheads*). WGA (*blue*) labels tracheal cell surfaces. *G*, in st16 embryos expressing a UAS-Serp(CBD)-GFP transgene (10) in tracheal cells (*breathless*GAL4) Serp-GFP, detected by anti-GFP co-localizes with Obst-A. *H* and *I*, in st14 and st16 heterozygous *obst-A* control embryos, Knk is enriched in the tracheal lumen. *J* and *K*, in st14 *obst-A*-null mutants Knk is enriched in the tracheal lumen, but is strongly reduced at st16 (*arrowheads*). *L*, transheterozygous mutants bearing single copy alleles of *serp*, *verm*, and *obst-A* show Knk reduction in the tracheal lumen at st16. Single channels are shown in *gray*. Scale bars represent 10 μm. *M*, *in vitro* interaction assay, Knk is pulled down by the GST-Obst-A fusion protein from *wt* embryo extract. *Asterisks* indicate GST, GST-Obst-A and Knk. *N*, schematic representation indicating the role of Obst-A in preventing cuticle degradation. Obst-A binds to chitin for cuticular localization and provides a scaffold for interaction and coordinating Knk and Serp presence in the ECM. The resulting Obst-A complex protects chitin from premature degradation. Loss of Obst-A disrupts Knk-mediated chitin protection from chitinase action, which may result in access of chitinolytic enzymes responsible for chitin ECM degradation.

We observed in *obst-A* mutants irregular Serp degradation in areas of the luminal ECM, where chitin appeared unaffected and might be subsequently degraded (supplemental Fig. S7*D*). Additionally, immunolabeling revealed co-localization of Obst-A and UAS-GAL4 mediated expression of Serp(CBD)-GFP (10) in the tracheal lumina (Fig. 6*G*). Altogether, these findings show that Obst-A complexes with the chitin modifier Serp at the extracellular matrix independently from chitin. This further demonstrates the requirement of Obst-A to control Serp in the ECM, which is essential to preserve the tracheal chitin matrix structure and to control tube size.

As Obst-A and Serp provide a scaffold to coordinate chitin matrix properties, it may interact with components involved in protecting the cuticle from degradation, such as Knk (8). Confocal analysis of immunolabeling studies in control embryos revealed Knk accumulation in the tracheal tube lumina starting from st14 until st16 (Fig. 6, *H* and *I*). In contrast, already accumulated luminal Knk was reduced at st16 in *obst-A* mutant embryos (Fig. 6, *J* and *K*). Our data show that Obst-A is required for the presence of Knk in the luminal chitin ECM. Moreover, this was also the case in a genetic interaction test. The 50% reduction of *obst-A*, *serp* and *verm* in transheterozygous animals, combining only single heterozygous mutant alleles (*obst-A*/+; *serp,verm*/+), revealed luminal Knk depletion, which was not the case in heterozygous control animals (Fig. 6, *H* and *L*). Previously it was shown that the *knk* down-regulation and mutation led to reduced chitin levels (7, 8). Consistently, irregular reduction of Knk resulted in a premature chitin degradation in *obst-A*-null and transheterozygous mutants (Fig. 6, *K* and *L*). Additionally, pull-down assays revealed co-precipitation of the GST-Obst-A fusion protein with Knk from embryo lysate, while GST alone did not (Fig. 6*M*; supplemental Fig. S6*D*). In summary, these findings indicate that Obst-A controls the presence of Knk in the cuticle for coordinating protection of chitin ECM from premature degradation.

DISCUSSION

We have analyzed the molecular process of chitin ECM dynamics in *Drosophila*. Our studies demonstrate the specific requirement of Obst-A for chitin ECM protection. We show that Obst-A binds and co-localizes with chitin in cuticle forming organs. Additionally, Obst-A interacts with Serp and Knk forming a core complex with chitin. Serp preserves the cuticle structure (10, 11) and Knk organizes chitin and protects it from chitinases (7, 8). Mutant studies demonstrate that Obst-A is required to control Serp and Knk presence in the cuticle. The premature reduction of Serp and Knk in *obst-A* mutants was independent from chitin. Genetic studies further show that Obst-A and Serp may interact to control the Knk localization for chitin protection. We propose that Obst-A is required to form a core complex in the chitin ECM that coordinates Knk presence for protecting chitin from premature degradation (Fig. 6*N*). Consistent with previous observations (7, 8, 10, 11), our findings suggest that Obst-A coordinated chitin ECM protection is required for tracheal tube expansion and presumably for cuticle function during development.

ECM is involved in organizing proper tube expansion which is vital for transport of liquids and gases across the body (26). The organization of distinct branches and the tracheal epithelium are determinants of tube size. Furthermore, apical secretion of chitin matrix components into the forming lumina is involved in uniform tracheal tube expansion. Chitin modifications and filament structure are involved in tube length control (5, 27). Our studies demonstrate that chitin ECM protection organized by Obst-A at st16 is required to coordinate tube size. We found that the lack of Obst-A resulted in tracheal overexpansion. Obst-A is expressed in tracheal cells and secreted towards the developing tube lumina where it co-localizes and interacts with the ECM core components chitin, Serp, and Knk. Additionally, *obst-A*-null mutants studies showed that apical matrix components started to degrade irregularly from tracheal tube lumina. These findings suggest that Obst-A is required to prevent a premature degradation of the luminal ECM thereby providing a matrix for determining final tube size at late embryogenesis.

The cuticle is one of the most abundant ECM structures in nature. It is common among arthropods and serves as an exoskeleton throughout their lifetime that accommodates growth. It further provides a protective layer against mechanical, physical and chemical stress (1–4, 8, 20, 28, 29). The chitin ECM lines epithelial cells of the epidermis, spiracles, trachea, and parts of the digestive tract. The dynamic organization of ECM during cuticle molting in these organs is poorly understood. Our studies demonstrate the importance of Obst-A for molting. Obst-A co-localized with core ECM components of epidermis, head skeleton, trachea, foregut, and posterior spiracles. Loss of *obst-A* resulted in severe cuticle integrity, structure, and molting defects in these organs. Additionally, *obst-A* mutants showed larval growth arrest and lethality. We showed that the impaired ECM protection in *obst-A* mutants resulted in a premature degradation of the luminal matrix of trachea. We assume that Obst-A mediated ECM protection could also affect Obst-A expressing, cuticle forming organs, such as the epidermal exoskeleton. However, it remains elusive whether the defective ECM protection causes cuticle molting defects observed in the *obst-A* mutants. It is interesting to note that Serp and Knk are evolutionarily conserved (8–11). Importantly, Obst-A homologs were identified in arthropods and nematodes (Fig. 2*C*) (12, 30). This suggests that a similar mechanism may exist to control chitin ECM degradation among chitinous invertebrates.

Acknowledgments—We thank Stefan Luschnig, Bernard Moussian, and Anne Uv for sharing flies and reagents. We thank Anna C. Aschenbrenner, Andreas Fink, Michael Hoch, Tamara Krsmanovic, and Christian Wolf for comments on the manuscript. We appreciate experimental assistance by Nataliya Nedzhvestkaya, Sabine Büttner, and Birgit Stümpges. We thank Michael Hoch for support.

REFERENCES

1. Galko, M. J., and Krasnow, M. A. (2004) Cellular and genetic analysis of wound healing in *Drosophila* larvae. *PLoS Biol.* **2,** E239
2. Chang, E. S. (1993) Comparative endocrinology of molting and reproduction: insects and crustaceans. *Annu. Rev. Entomol.* **38,** 161–180
3. Merzendorfer, H., and Zimoch, L. (2003) Chitin metabolism in insects: structure, function and regulation of chitin synthases and chitinases. *J. Exp. Biol.* **206,** 4393–4412
4. Moussian, B. (2010) Recent advances in understanding mechanisms of insect cuticle differentiation. *Insect Biochem. Mol. Biol.* **40,** 363–375
5. Affolter, M., and Caussinus, E. (2008) Tracheal branching morphogenesis in *Drosophila*: new insights into cell behavior and organ architecture. *Development* **135,** 2055–2064
6. Behr, M. (2010) Molecular aspects of respiratory and vascular tube development. *Respir. Physiol. Neurobiol.* **173,** S33–36
7. Moussian, B., Tång, E., Tonning, A., Helms, S., Schwarz, H., Nüsslein-Volhard, C., and Uv, A. E. (2006) *Drosophila* Knickkopf and Retroactive are needed for epithelial tube growth and cuticle differentiation through their specific requirement for chitin filament organization. *Development* **133,** 163–171
8. Chaudhari, S. S., Arakane, Y., Specht, C. A., Moussian, B., Boyle, D. L., Park, Y., Kramer, K. J., Beeman, R. W., and Muthukrishnan, S. (2011) Knickkopf protein protects and organizes chitin in the newly synthesized insect exoskeleton. *Proc. Natl. Acad. Sci. U.S.A.* **108,** 17028–17033
9. Dixit, R., Arakane, Y., Specht, C. A., Richard, C., Kramer, K. J., Beeman, R. W., and Muthukrishnan, S. (2008) Domain organization and phylogenetic analysis of proteins from the chitin deacetylase gene family of *Tribolium castaneum* and three other species of insects. *Insect Biochem. Mol. Biol.* **38,** 440–451
10. Luschnig, S., Bätz, T., Armbruster, K., and Krasnow, M. A. (2006) Serpentine and vermiform encode matrix proteins with chitin binding and deacetylation domains that limit tracheal tube length in *Drosophila*. *Curr. Biol.* **16,** 186–194
11. Wang, S., Jayaram, S. A., Hemphälä, J., Senti, K. A., Tsarouhas, V., Jin, H., and Samakovlis, C. (2006) Septate-junction-dependent luminal deposition of chitin deacetylases restricts tube elongation in the *Drosophila* trachea. *Curr. Biol.* **16,** 180–185
12. Behr, M., and Hoch, M. (2005) Identification of the novel evolutionary conserved obstructor multigene family in invertebrates. *FEBS Lett.* **579,** 6827–6833
13. Parks, A. L., Cook, K. R., Belvin, M., Dompe, N. A., Fawcett, R., Huppert, K., Tan, L. R., Winter, C. G., Bogart, K. P, Deal, J. E., Deal-Herr, M. E., Grant, D., Marcinko, M., Miyazaki, W. Y., Robertson, S., Shaw, K. J., Tabios, M., Vysotskaia, V., Zhao, L., Andrade, R. S., Edgar, K. A., Howie, E., Killpack, K., Milash, B., Norton, A., Thao, D., Whittaker, K., Winner, M. A., Friedman, L., Margolis, J., Singer, M. A., Kopczynski, C., Curtis, D., Kaufman, T. C., Plowman, G. D., Duyk, G., and Francis-Lang, H. L. (2004) Systematic generation of high-resolution deletion coverage of the *Dro-*

sophila melanogaster genome. *Nat. Genet.* **36,** 288–292
14. Tonning, A., Hemphälä, J., Tång, E., Nannmark, U., Samakovlis, C., and Uv, A. (2005) A transient luminal chitinous matrix is required to model epithelial tube diameter in the *Drosophila* trachea. *Dev. Cell* **9,** 423–430
15. Wingen, C., Stümpges, B., Hoch, M., Behr, M. (2009) Expression and localization of clathrin heavy chain in *Drosophila melanogaster*. *Gene Expr. Patterns.* **9,** 549–554
16. Nisole, A., Stewart, D., Bowman, S., Zhang, D., Krell, P. J., Doucet, D., and Cusson, M. (2010) Cloning and characterization of a Gasp homolog from the spruce budworm, *Choristoneura fumiferana*, and its putative role in cuticle formation. *J. Insect Physiol.* **56,** 1427–1435
17. Bauer, R., Lehmann, C., Fuss, B., Eckardt, F., and Hoch, M. (2002) The *Drosophila* gap junction channel gene innexin 2 controls foregut development in response to Wingless signaling. *J. Cell Sci.* **115,** 1859–1867
18. Tamura, K., Peterson, D., Peterson, N., Stecher, G., Nei, M., Kumar, S. (2011) MEGA5: molecular evolutionary genetics analysis using maximum likelihood, evolutionary distance, and maximum parsimony methods. *Mol. Biol. Evol.* **28,** 2731–2739
19. Li, T., and Bender, M. (2000) A conditional rescue system reveals essential functions for the ecdysone receptor (EcR) gene during molting and metamorphosis in *Drosophila*. *Development* **127,** 2897–2905
20. Zhu, Q., Arakane, Y., Beeman, R. W., Kramer, K. J., and Muthukrishnan, S. (2008) Functional specialization among insect chitinase family genes revealed by RNA interference. *Proc. Natl. Acad. Sci. U.S.A.* **105,** 6650–6655
21. Behr, M., Wingen, C., Wolf, C., Schuh, R., and Hoch, M. (2007) Wurst is essential for airway clearance and respiratory-tube size control. *Nat. Cell Biol.* **9,** 847–853
22. Stümpges, B., and Behr, M. (2011) Time-specific regulation of airway clearance by the *Drosophila* J-domain transmembrane protein Wurst. *FEBS Lett.* **585,** 3316–3321
23. Tsarouhas, V., Senti, K. A., Jayaram, S. A., Tiklová, K., Hemphälä, J., Adler, J., and Samakovlis, C. (2007) Sequential pulses of apical epithelial secretion and endocytosis drive airway maturation in *Drosophila*. *Dev. Cell* **13,** 214–225
24. Behr, M., Riedel, D., and Schuh, R. (2003) The claudin-like Megatrachea is essential in septate junctions for the epithelial barrier function in *Drosophila*. *Dev. Cell* **5,** 611–620
25. Lamb, R. S., Ward, R. E., Schweizer, L., and Fehon, R. G. (1998) *Drosophila coracle*, a member of the protein 4.1 superfamily, has essential structural functions in the septate junctions and developmental functions in embryonic and adult epithelial cells. *Mol. Biol. Cell* **9,** 3505–3519
26. Bryant, D. M., and Mostov, K. E. (2008) From cells to organs: building polarized tissue. *Nat. Rev. Mol. Cell Biol.* **9,** 887–901
27. Casanova J. (2007) The emergence of shape: notions from the study of the *Drosophila* tracheal system. *EMBO Rep.* **8,** 335–339
28. Chavoshi, T. M., Moussian, B., and Uv, A. (2010) Tissue-autonomous EcR functions are required for concurrent organ morphogenesis in the *Drosophila* embryo. *Mech. Dev.* **127,** 308–319
29. Guan, X., Middlebrooks, B. W., Alexander, S., and Wasserman, S. A. (2006) Mutation of TweedleD, a member of an unconventional cuticle protein family, alters body shape in *Drosophila*. *Proc. Natl. Acad. Sci. U.S.A.* **103,** 16794–16799
30. Jasrapuria, S., Arakane, Y., Osman, G., Kramer, K. J., Beeman, R. W., and Muthukrishnan, S. (2010) Genes encoding proteins with peritrophin A-type chitin-binding domains in *Tribolium castaneum* are grouped into three distinct families based on phylogeny, expression and function. *Insect Biochem. Mol. Biol.* **40,** 214–227